Research Academy for Young Scientists

Describing and Modeling Ocean Waves Using Linear and Non-linear Wave Theories

Algot Kullberg
algotkullberg@icloud.com

under the direction of
Parvathy Kunchi Kannan
KTH Royal Institute of Technology
Department of Fluid Mechanics

July 12, 2023

*

Abstract

The damages caused on offshore structures due to wave loading can be minimized through modelling and predicting the surface elevation and kinematics of ocean waves. The most utilized model is the Linear Random Wave Theory (LRWT), although there are empirically corrected models and non-linear models which are more realistic. Linear and non-linear wave models have been compared before, and this study aims to validate the previous results. This is done through a comparison between LRWT, a second order Random Wave Theory, Stokes wave theory and measured wave data of surface elevation, as well as a comparison of the velocities predicted by the mentioned models and Wheeler stretching. The results contradicts those of previous studies in that the linear wave model described the surface elevation the most accurately. However, it is concluded that the second order wave theory is more applicable in describing wave kinematics. Further studies are needed to better distinguish between free, wind-generated waves, and bound waves, which stem from the interaction between free waves. This would greatly improve the predictions made by the second order wave theory.

Acknowledgements

Firstly, I would like to thank my mentor Parvathy for two fantastic weeks at KTH Royal Institute of Technology. They have been highly inspiring and fulfilling. I would also like to thank my project partner Tingxuan Dai for the countless hours of discussion and for the invaluable companionship, which cannot be emphasized enough. Finally, this project would not have been possible without the amazing Rays – for excellence team and contributing partners Stiftelsen Oscar Hrischs Minne and Beijerstiftelsen.

Contents

Glossary

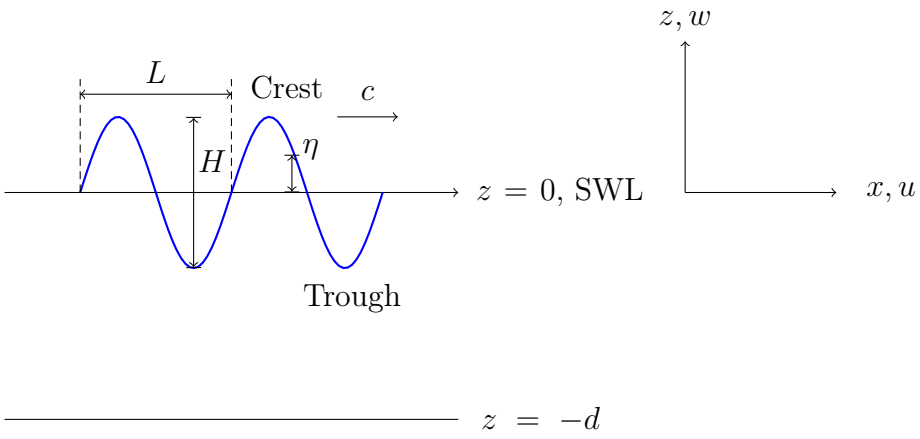

Table 1: Symbols with explanations and units

Symbol	Explanation	Unit
H	wave height	[m]
$a = \frac{H}{2}$	amplitude	[m]
L	wavelength	[m]
$s = \frac{H}{L}$	wave steepness	-
T	wave period	[s^{-1}]
d	water depth	[m]
η	water surface elevation	[m]
$c = \frac{L}{T}$	phase speed	[m/s]
u	velocity component in direction of travel	[m/s]
w	velocity component perpendicular to direction of travel	[m/s]
x	horizontal axis	-
z	vertical axis	-
$k = \frac{2\pi}{L}$	wave number	[m^{-1}]
$\omega = \frac{2\pi}{T}$	wave frequency	[s^{-1}]
$f = \frac{1}{T}$	frequency	[s^{-1}]
α	phase angle	[rad]
SWL	Still Water Level	-

1 Introduction

For an offshore structure such as a wind turbine or oil platform, wind generated random waves cause vast damages [1]. Waves hit the structure in pulses, where the pressure differences cause large stresses. In addition, fatigue damage to the hull is one of the most severe problems that large ships suffer from. In order to minimize wave loads, it is crucial to understand and model the characteristics of wave elevation and wave kinematics. This is commonly done with Linear Random Wave Theory (LRWT), which gives a simple description of ocean waves as a sum of cosine waves. However, the theory overestimates the horizontal velocities close to the surface and poorly models surface elevation of steep waves. Instead, empirical corrections and non-linear models are used to better model near-surface kinematics [1].

This paper gives a description of different theories of water waves. Additionally, the behaviour of water waves is investigated, as well as how they can be modeled using LRWT [2], Wheeler stretching [3], Stokes' expansion [4] and a second order Random Wave Theory proposed by Sharma and Dean [5]. This is done by comparing the different theories to real ocean wave data collected by Prof. Chris Swam and Dr. Adrian Callaghan [6]. The study is focused on extreme events, i.e the tallest crest of a wave train. Moreover, the measured surface elevation is dependent on time t, and independent of horizontal displacement x.

1.1 Description of Water Waves

Water waves are deformations of the water surface, transporting energy in the direction of travel. Their energy originates from the sun, which heats the air causing wind to blow due to the pressure gradient. The wind transfers its energy to the water through friction, which creates waves. The waves grow as the transferred energy increases with larger wave height. When sufficiently big, the pressure differences between the sheltered lee side of the wave and the wind side further enlarges the wave. However, waves are not dependent on the wind to propagate: once they are formed, they can travel unaided [7].

The wind-blown sea surface is characterized by irregular waves since the waves travel at different speeds and different direction, and since the smaller waves are superimposed as

ripples on the larger waves [8]. Water waves can be divided into long-crested, unidirectional waves, and short-crested, multidirectional waves [2]. When applying the theories in this study, the waves are assumed to be long-crested.

Additionally, water waves are categorized into deep water waves, intermediate water waves and shallow water waves, depending on the relation between wavelength and water depth. For deep water waves $d > \frac{1}{2}L$, and for shallow water waves $d < \frac{1}{20}L$ [9]. The collected data presented in this paper is from deep water waves, and the depth is assumed to be infinite.

1.2 Regular Waves

Linear wave theory gives a description of waves using linearised equations and is explained in detail in [2]. Linear regular waves only have one wave component and are steady, i.e periodic. However, the theory only holds true under a set of assumptions.

1.2.1 Assumptions

In Linear wave theory it is assumed that the fluid is incompressible, which implies that

$$\nabla \cdot v = 0, \tag{1}$$

where v is the velocity field such that $v = (u, w)$. Here, u is horizontal fluid velocity and w is the vertical fluid velocity. In addition, motion is irrotational, which is expressed as

$$\nabla \times v = 0. \tag{2}$$

Moreover, the wave motion is assumed to be periodic in horizontal position x and time t, which means that the wave height η varies in a pattern over a wavelength or a wave period. Lastly, it is assumed that the steepness of the wave is low, $s \ll 1$, and that the amplitude is small compared to the water depth, $a \ll d$. This is because (1) high wave steepness causes non-linear terms to become significant, thus invalidating the Linear wave theory, and (2) the influence of the water bed has to be negligible in order for the Linear

wave theory to apply [2].

1.2.2 Governing Equation

The governing equation of Linear wave theory is the Laplace Equation stating that

$$\nabla^2 \cdot v = 0. \tag{3}$$

As a result of the periodicity assumption together with Equation (3), the horizontal and vertical velocity components are approximated to

$$u = [A\cosh(kz) + B\sinh(kz)]\sin(\omega t - kx) \tag{4}$$

and

$$w = [A\sinh(kz) + B\cosh(kz)]\cos(\omega t - kx) \tag{5}$$

where A and B are determined using boundary conditions.

1.2.3 Boundary Conditions

The boundary layer is defined as a layer of fluid that is influenced by viscous forces, i.e forces that resist shearing motion. According to the no-slip boundary condition, the horizontal fluid velocity is specified to be zero at the sea bed, $u = 0$ at $z = -d$. In addition, the vertical velocity must be zero at the bed since particles cannot permeate the sea bed, $w = 0$ at $z = -d$. This is known as the Bottom Boundary Condition (BBC) [8]. Additionally, it has to be assumed that the control volume on the surface remains on the surface. The vertical velocity component is thus equal to the change of the surface elevation evaluated at the surface. This is known as the Kinematic Free Surface Boundary Condition (KFSBC) [2] and states that

$$\frac{d\eta}{dt} = \frac{\partial \eta}{\partial t} + \frac{\partial \eta}{\partial x}\frac{dx}{dt} = w\,|_{z=\eta} \tag{6}$$

However, since the waves are assumed to be of small amplitude, the velocity at the surface is approximately equal to the velocity at the SWL [8]. Using this and ignoring second order terms, Equation (6) can be rewritten as

$$\frac{\partial \eta}{\partial t} \approx w\,|_{z=0}\ . \tag{7}$$

From this relationship together with Equation (5), it is found that surface elevation, η can be expressed as

$$\eta = a\sin(\omega t - kx). \tag{8}$$

.

1.2.4 Phase Velocity and Dispersion

The phase velocity is the speed of individual waves. To find the phase velocity $c = \frac{L}{T}$, the dispersion relationship is utilized. It states that

$$\omega^2 = gk\ \tanh(kd). \tag{9}$$

Followed from Equation (9), the phase velocity is given by

$$c = \frac{L}{T} = \frac{\omega}{k} = \left[\frac{g}{k}\tanh(kd)\right]^{1/2} \tag{10}$$

or equivalently,

$$c = \left[\frac{gL}{2\pi}\tanh\left(\frac{2\pi d}{L}\right)\right]^{1/2}. \tag{11}$$

This indicates that waves with different wavelength travel at different phase velocities. In addition, Equation (9) can be rewritten in terms of the wavelength $L = \frac{2\pi}{\omega}$ as

$$L = \frac{gT^2}{2\pi}\tanh\frac{2\pi d}{L}. \tag{12}$$

In this equation, it is impossible to solve for L analytically [9]. However, there are approximations such as the following:

$$L = \frac{2\pi d}{x^2(1 - exp(-x^\beta))^{-1/\beta}}, \tag{13}$$

where $x = \omega d/\sqrt{gd}$ and $\beta = 2.4908$ [10]. This can be used as a first estimation when computing L through an iterative process [9].

1.2.5 Wave Energy

The total energy of a wave consists of potential energy from the location of a control volume, and kinetic energy from the motion of control volumes. The total wave energy is given as

$$\mathrm{E} = \rho\frac{ga^2}{2}, \tag{14}$$

where ρ is the fluid density, g is the gravitational constant and a is the wave amplitude. Hence, the wave energy is proportional to the amplitude squared [9].

1.2.6 Stokes' Wave Theory

Despite the linear regular wave theory providing a simple description of regular waves, water waves generated in large labs seldom follow the Linear wave theory presented in section 1.2. The reason is that the waves are non-linear, which means that they are a sum of several waves. The number of terms determines the order of the wave, which is important since the higher order terms play a significant role when the waves get steeper [4].

A more realistic description can be found with Stokes' waves [4]. The theory provides a description of non-linear waves by adding cosine waves with increasing frequency (see Appendix A). The different wave components are called harmonics, where the linear component is the first harmonic. By definition, the first harmonic is a first order Stokes wave. Higher order Stokes' waves generally have taller crests and broader, less deep troughs, as can be seen in Figure 1 [8].

Different orders of Stokes' waves, i.e different number of wave components, are valid for specific spectra of wave heights and water depths. The first order theory is only valid

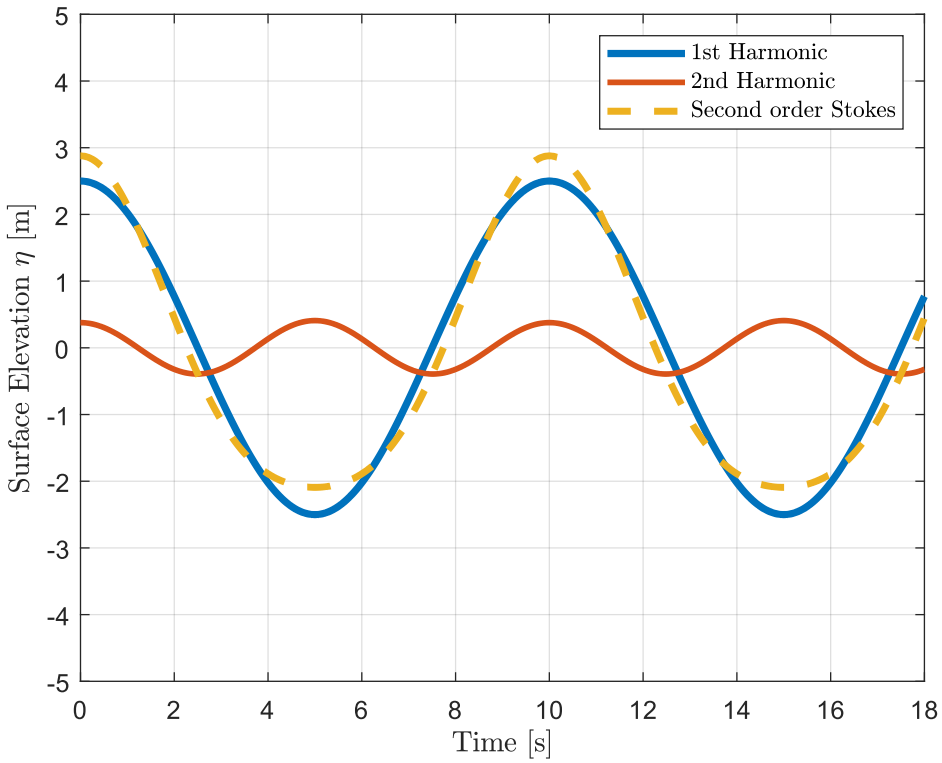

Figure 1: Illustration of a second order wave. The Stokes' wave is a sum of the 1st and 2nd Harmonic.

for a certain range of small wave heights and great water depths, while the Stokes' fifth order is applicable over a wider range of wave heights [9].

1.3 Random Waves

In the linear and non-linear wave theories described above the wave train is periodic and has a constant phase velocity. However, real ocean are unsteady, meaning that they are irregular and random [8].

1.3.1 Linear Random Wave Theory

Linear random waves can be described as a sum of linear waves with *random* phase angles, α. This is expressed as a sum of several free waves:

$$\eta(x,t) = \sum_{m=1}^{\infty} a_m \cos(k_m x - \omega_m t + \alpha_m), \tag{15}$$

where the index m corresponds to the m^{th} wave component. Importantly, the peak frequency ω_p is the frequency corresponding to the highest amplitude [11].

Due to the unsteady properties of random waves, statistical tools need to be utilized in order to predict the behavior of waves. Instead of considering the individual waves, measurements of the wave spectrum are used. One such measurement is the significant wave height H_s, which is the average height of the highest third of the waves. It has been found that H_s correlates with the visual impression of the wave height [8]. In addition,

$$H_s \approx 4\sigma \tag{16}$$

where σ is the standard deviation of the wave heights.

In random waves, the wave period is based on zero down-crossing, which means that the wave period is the time interval between two subsequent crossings of the SWL from above. The height is the difference between the maximum value of η and the minimum value of η in a given wave period. When using zero down-crossing, the wave height is measured in the direction of travel. This is used since the greatest force often is experienced when the wave front hits the structure [9].

1.3.2 Wheeler Stretching

The random wave system is decomposed into a large number of linear waves, commonly using Fourier decomposition [2]. However, the effects of interactions between waves are not taken into consideration. Together with other simplifications, such as the KFSBC applied at the SWL in Equation (7), this causes the LRWT to over-predict the horizontal velocity above SWL. This can be seen in the expression for u in Equation (4) when assuming deep water depth and short wavelength, as is the case for higher frequency terms. Then, k is large and Equation (4) can be rewritten as:

$$u = a\omega e^{kz} \cos(\omega t + \alpha), \tag{17}$$

where u is independent of horizontal displacement x [1]. For negative z values (under SWL), e^{kz} is smaller than unity. However, it increases significantly for large k and z values, which causes large errors in the predicted velocity. This is referred to as high-frequency contamination and means that the horizontal velocities below the wave crest are over-predicted [1].

In order to create more accurate approximations, various empirically corrected linear wave theories have been developed. The most widely utilized empirically corrected theory is the Wheeler stretching theory [3]. Wheeler stretching sets the zero point of vertical location, z, to the surface elevation so that the velocity predictions are shifted. This is done through the change of z-coordinate from z to z^*, where

$$z^* = \frac{z - \eta}{1 + \frac{\eta}{d}} \tag{18}$$

1.3.3 Second Order Random Wave Theory

An alternative procedure of finding a more realistic velocity profile is through considering the non-linearity of the random water waves. For random waves, non-linearity represents the interactions between waves, which is also called wave coupling. An analytical solution to non-linear two-wave interactions is defined by Longuet-Higgins and Stewart [12] as

$$\eta = \eta_1 + \eta_2 + \frac{a_1 a_2}{2g}\{\mathrm{C}\cos(\psi_1 - \psi_2) - \mathrm{D}\cos(\psi_1 + \psi_2)\}, \tag{19}$$

where

$$\psi_1 = (k_1 x - \omega_1 t)\ ;\ \psi_2 = (k_2 x - \omega_2 t) \tag{20}$$

and C and D are defined in terms of ω, k and d (see Appendix B). In Equation (27), η_1 represents the first free wave and η_2 is the second free wave. The third term is called a bound wave. LRWT assumes that all waves are free waves and apply the dispersion relationship to all components, although bound waves do not satisfy the dispersion relationship [13]. Taking this into account, random waves can be described by a second order random wave theory, which considers all possible interactions between two free waves. The first solution

was proposed by Sharma and Dean [5] and is based on the previous theory by Longuet-Higgins and Stewart. The equation for the second order RWT can be found in Appendix C. It should be mentioned that the use of second order wave theory requires free waves, and not bound waves, as input since the creation of bound waves is inherent in the model. When measured field data is decomposed into a superposition of linear components, the result consists of both free and bound waves. In order to distinguish between the two, one may consider the frequency of high amplitude bound waves. Generally, bound waves have smaller amplitude than the free waves for frequencies around the spectral peak and tend to be dominant in frequencies either much higher or lower than the spectral peak. In addition, free waves are dominant in almost the entire frequency spectrum in waves that are not steep. To exclude high-frequency bound waves, a cut-off frequency can be defined, which is the highest frequency included in the input spectrum [13].

1.4 Previous Studies

Zhang et al [14, 15] compared the LRWT, Wheeler stretching and a hybrid second order random wave model to describe the elevation and velocity of lab made water waves. The hybrid second order random wave model differs from that of Sharma and Dean in also considering phase modulation, which better separates free waves from bound waves. Regarding the surface elevation, the hybrid model was the most accurate, especially in steep waves. Furthermore, the study found that the hybrid model described the velocity profile the most accurately, followed by Wheeler stretching. This was especially true for steep waves. On the other hand, LRWT greatly overestimated the velocity above SWL.

These results were replicated in [16] where a similar relation between the velocity profiles predicted by LRWT, Wheeler stretching and a second order random wave model was found. In particular, the second order RWT followed the measured velocity closely. The study also investigated a regular, periodic wave theory called Grue's method, similar to that of Stokes' third order waves. The method accurately described the horizontal velocity component for $z > 0$, although over-predicting the velocity for $z < 0$. However, it is concluded that the model only may be used on one crest at a time due to its peri-

odicity. [16]. Another study [13] found that LRWT overestimates the trough heights and underestimates the crest heights. It was also confirmed that a hybrid second order model describes the surface elevation more accurately than LRWT.

1.5 Aim of Study

The aim of this study was to validate the precision of LRWT, Wheeler stretching, Stokes' fifth order expansion and a second order RWT by Sharma and Dean in approximating the surface elevation around and velocity profile under the tallest crest of a random ocean wave. This is done through a comparison with measured data of surface elevation around the highest crest.

2 Method

Ocean wave data of surface elevation over a time span of 100 seconds was collected by Prof Chris Swam and Dr Adrian Callaghan [6]. The surface elevation over the entire time span is shown in Figure 2a and the wave period with the highest wave crest can be seen in Figure 2b. The amplitudes corresponding to the different frequencies is shown in Figure 3.

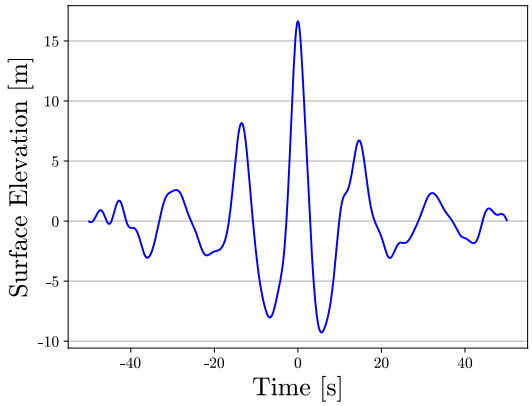

(a) Measured surface elevation η over time $-50 < t < 50$.

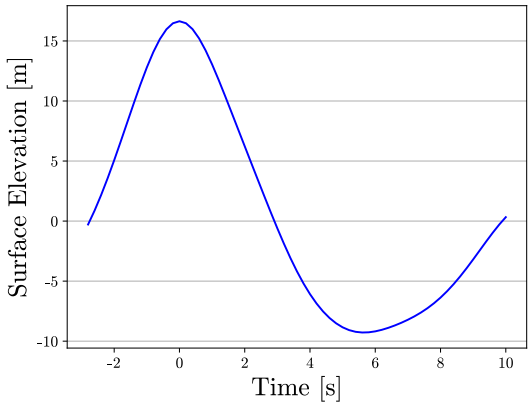

(b) Measured surface elevation η over the wave period corresponding to the highest crest, $-2.8 < t < 10$.

The frequencies and corresponding amplitudes and phase angles were extrapolated through

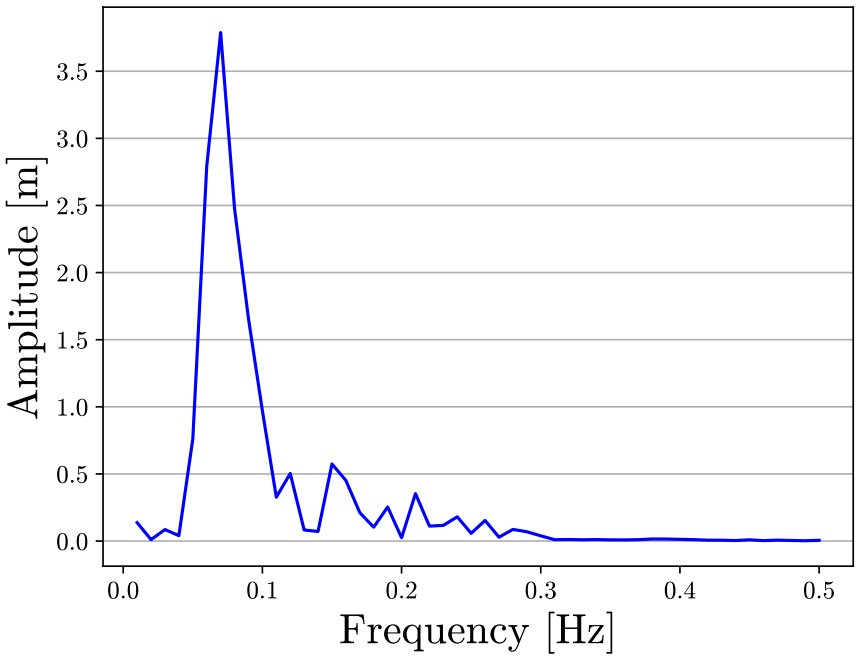

Figure 3: Amplitude-frequency spectrum.

Fourier decomposition of the random wave into fifty wave components, and the wavelengths were found using the dispersion equation. The details of the decomposition, such as whether the phase angles were generated randomly, is unknown as it is not specified in the data retrieved from Prof. Swam and Dr. Callaghan [6].

Afterwards, the significant and maximum wave height was determined with zero-down crossing. The wave period with the maximum surface elevation was used as a reference since it carries the most energy (see Figure 2b). Subsequently, LRWT, Stokes' expansion and the second order RWT by Sharma and Dean was used to find the surface elevation, η. The input frequency spectra for the second order RWT was determined using a low-pass filter with the cut-off frequency

$$f_{cut} = \sqrt{\frac{2g}{H_s}}, \tag{21}$$

where $g = 9.81\,\mathrm{m/s^2}$ is the gravitational constant, H_s is the significant wave height and $f = \frac{\omega}{2\pi}$ [17]. This gave $f_{cut} = 0.17\,\mathrm{Hz}$.

Lastly, the velocity component in the direction of propagation u as a function of the depth z under the highest crest was found using the theories above together with Wheeler

stretching. From this, the maximum predicted velocity was calculated.

3 Results

The modeled surface elevations can be seen in Figure 4 and the corresponding R^2 values are shown in Table 2. The order of Stokes' waves was chosen to be five, in order to be sufficient in describing a steep wave. The steepness of the highest crest was approximated to $s = 0.042$ using Equation (13).

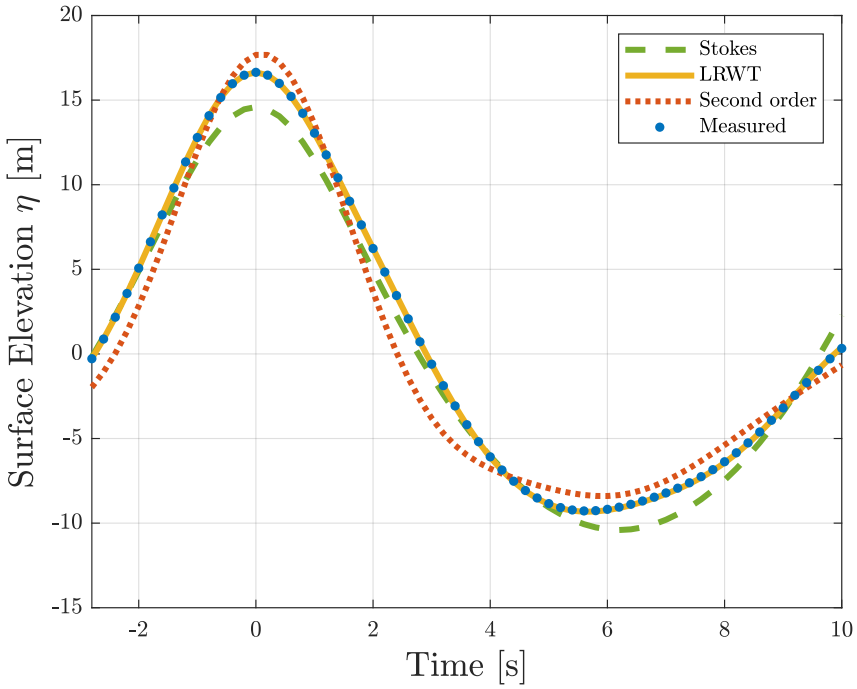

Figure 4: Surface elevation η calculated using second order RWT (in red). Stokes' fifth order (in green), LRWT (in yellow), compared against measured data (blue dots).

Table 2: R^2 values for surface elevation at $-2.8 < t < 10$ of the different models.

Model	R^2
LRWT	1.000
Second Order RWT	0.971
Stokes	0.983

In addition, Figure 5 shows the velocities on a given depth z under the highest crest (where t = 0), determined by LRWT, Wheeler Stretching, Stokes fifth order expansion

and the second order RWT. The maximum velocities predicted by the different models are shown in Table 3.

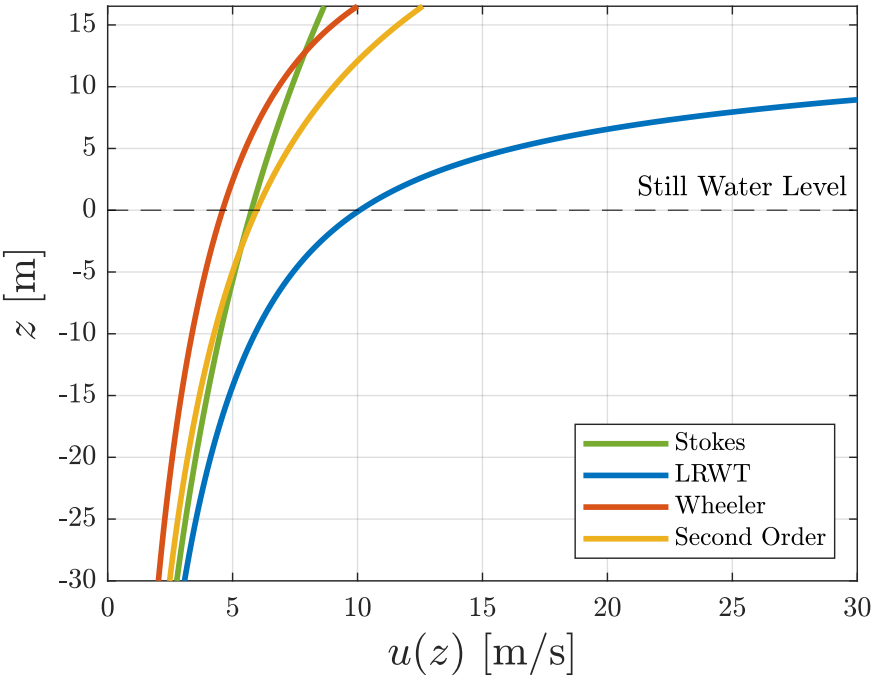

Figure 5: Velocities under the highest crest (t = 0) predicted by LRWT (in blue), Wheeler stretching (in red), second order RWT (in yellow) and Stokes fifth order (in green). The velocity is calculated from water depth $z = -80\,\mathrm{m}$ to the wave surface $z = 16.6\,\mathrm{m}$.

Table 3: Velocity calculated with different models at η_{max}, $z = 16.6\,\mathrm{m}$

Model	Velocity [m/s]
LRWT	5.48×10^5
Wheeler's Stretching	10.2
Second Order RWT	12.7
Stokes	8.69

Furthermore, the maximum surface elevation, significant wave height and peak frequency was found to be $\eta_{\max} = 16.6\,\mathrm{m}$, $H_s = 16.7\,\mathrm{m}$ and $f_p = 0.07\,\mathrm{Hz}$ respectively.

4 Discussion

The Linear Random Wave Theory (LRWT) modeled the measured surface elevation the best, although it predicted unrealistic velocities (in the order of $10^5\,\mathrm{m/s}$). On the other

hand, the other theories gave more reasonable velocities albeit not as accurate surface elevation.

4.1 Surface Elevation

Compared to other studies [13, 15], the LRWT fitted the measured surface elevation surprisingly well, even considerably better than the second order wave model (see Table 2). The reason for this is that the input of the LRWT is based on a Fourier decomposition of the very same data. Per definition, this will produce a wave closely equivalent to the one serving as input. It is likely that the phase angles were determined to fit the data and not chosen randomly, which causes the LRWT to be overfitted. Moreover, the second order wave theory performed considerably worse than LRWT in modeling the surface elevation, which deviates from previous results. This is partly since the LRWT fitted the measured data so well. However, it could also be due to the difficulty of separating free waves from bound waves. If bound waves serve as input to the second order RWT, they cause the model to predict bound waves that do not exist.

In addition, no three wave (or higher order) coupling is considered. It is possible that a significant amount of bound waves were a product of higher order wave interactions. The steepness of the highest crest $s = 0.042\,\mathrm{m}$ is rather large ($s << 1$ does not apply) which could be a reason for the bound waves to be near the spectral peak and thus hard to exclude. Furthermore, the hybrid wave theory used in [15] utilizes a more precise procedure of identifying bound waves, whereas the frequency spectra in this study was chosen with an estimated cut-off frequency.

Regarding Stokes' waves, it should be mentioned that their regular nature makes them inapplicable over a wider range of random wave periods. However, they may acceptably well model a single wave period profile.

4.2 Horizontal Velocity

In alignment with previous studies [15, 16], the prediction of the horizontal velocity component under the highest crest is much higher by LRWT than by Wheeler stretching and

the second order RWT. Based on previous results [15, 16], the second order RWT may be the best approximation of the actual velocity profile, while LRWT predicts unrealistic velocities and Wheeler stretching and Stokes gives lower velocities. However, more precise conclusions on the accuracy of the different models would require measured data on the velocity, which was not included in this study.

4.3 Further Studies

This study focused on unidirectional waves. However, this is seldom relevant for real ocean waves as the directionality may affect the wave characteristics, such as the interactions between waves. Further studies should take into account the directional spread, i.e consider short-crested waves. In addition, the identification of bound waves is invaluable to the usage of higher order random waves and further development of the hybrid wave model, as well as higher order random wave theories would greatly increase the predictability of complex wave interactions.

4.4 Conclusion

In summary, the LRWT was found to accurately model the surface elevation, which may be due to a overfitted wave decomposition. However, the study finds similar velocity profiles to those of previous studies where the second order RWT offer more realistic predictions. All the same, the second order RWT is worse at approximating the surface elevation compared to previous studies. Thus, further research is needed to investigate how bound waves can be distinguished in order to improve the use of higher order theories.

References

[1] N. I. Mohd Zaki, M. K. Abu Husain, and G. Najafian, "Comparison of extreme responses from wheeler and vertical stretching methods," vol. 2, 06 2013.

[2] R. G. Dean and R. A. Dalrymple, *Water wave mechanics for engineers and scientists*, vol. 2. world scientific publishing company, 1991.

[3] J. Wheeler, "Method for calculating forces produced by irregular waves," *Journal of petroleum technology*, vol. 22, no. 03, pp. 359–367, 1970.

[4] M. Rahman, "Fundamentals concerning stokes waves," *WIT Transactions on Engineering Sciences*, vol. 9, 1970.

[5] J. Sharma and R. Dean, "Second-order directional seas and associated wave forces," *Society of Petroleum Engineers Journal*, vol. 21, no. 01, pp. 129–140, 1981.

[6] C. Swam and A. Callghan, "Mathematical modelling of ocean waves." 2020.

[7] R. Waters, *Energy from ocean waves: full scale experimental verification of a wave energy converter*. PhD thesis, Universitetsbiblioteket, 2008.

[8] P. Schöpfer, "Non-linear wave impact on monopile structures," 2016.

[9] T. L. Andersen and P. Frigaard, "Lecture notes for the course in water wave mechanics," 2011. `"https://vbn.aau.dk/ws/portalfiles/portal/205529532/Lecture_Notes_for_the_Course_in_Water_Wave_Mechanics.pdf"`.

[10] J. Guo, "Simple and explicit solution of wave dispersion equation," *Coastal Engineering*, vol. 45, no. 2, pp. 71–74, 2002.

[11] J.-B. Song, "Second-order random wave solutions for internal waves in a two-layer fluid," *Geophysical research letters*, vol. 31, no. 15, 2004.

[12] M. Longuet-Higgins and R. Stewart, "Changes in the form of short gravity waves on long waves and tidal currents," *Journal of Fluid Mechanics*, vol. 8, no. 4, pp. 565–583, 1960.

[13] J. Zhang, "Nonlinear wave interaction and its applications to the analysis of steep ocean waves," in *Rogue Waves 2000: Proceedings of a Workshop Organized by Ifremer and Held in Brest, France, 29-30 November 2000, Within de Brest SeaTechWeek 2000*, vol. 32, p. 91, Editions Quae, 2001.

[14] J. Zhang, L. Chen, M. Ye, and R. E. Randall, "Hybrid wave model for unidirectional irregular waves—part i. theory and numerical scheme," *Applied Ocean Research*, vol. 18, no. 2-3, pp. 77–92, 1996.

[15] C. Spell, J. Zhang, and R. E. Randall, "Hybrid wave model for unidirectional irregular waves—part ii. comparison with laboratory measurements," *Applied Ocean Research*, vol. 18, no. 2-3, pp. 93–110, 1996.

[16] C. Stansberg, O. Gudmestad, and S. Haver, "Kinematics under extreme waves," *Journal of Offshore Mechanics and Arctic Engineering-transactions of The Asme*, vol. 130, 05 2008.

[17] N. Veritas, *Environmental conditions and environmental loads*. Det Norske Veritas Oslo, Norway, 2000.

A Stokes Fifth Order Expansion

This appendix contains the equation for surface elevation, η and velocity potential function, ϕ using Stokes fifth order expansion. The velocity potential can be used to find the horizontal and vertical velocities as

$$\frac{\partial \phi}{\partial x} = u \tag{22}$$

and

$$\frac{\partial \phi}{\partial z} = w. \tag{23}$$

Surface elevation η is given from

$$\begin{aligned} k\eta(x) = kh + \epsilon\cos(kx) + \epsilon^2 B_{22}\cos(2kx) + \epsilon^3 B_{31}[\cos(kx) - \cos(3kx)] + \epsilon^4[B_{42}\cos(2kx) + B_{44}\cos(4kx)] \\ + \epsilon^5[-(B_{53}+B_{55})\cos(kx) + B_{53}\cos(3kx) + B_{55}\cos(5kx)] \end{aligned} \tag{24}$$

$$\phi(x,z) = -cx + c_o\left(\frac{g}{k^3}\right)^{\frac{1}{2}} \sum_{i=1}^{5} \epsilon^i \sum_{j=1}^{i} A_{ij}\cosh(jkz)\sin(jkx) \tag{25}$$

with $\epsilon = Hk/2$ and

$$\begin{aligned} B_{22} &= \coth(kh)\left(\frac{1+2S}{2(1-S)}\right) \\ B_{31} &= \frac{-3(1+3S+3S^2+2S^3)}{8(1-S)^3} \\ B_{42} &= \coth(kh)\frac{6-26S-182S^2-204S^3-25S^5+26S^5}{6(3+2S)(1-S)^4} \\ B_{44} &= \coth(kh)\frac{24+92S+122S^2+66S^3+67S^4+34S^5}{24(3+2S)(1-S)^4} \\ B_{53} &= 9\frac{132+17S-2.216S^2-5.897S^3-6.292S^4-2.687S^5+194S^6+467S^7+82S^8}{128(3+2S)(4+S)(1-S)^6} \\ B_{55} &= 5\frac{300+1.579S+3.176S^2+2.949S^3+1.188S^4+675S^5+1.326S^6+827S^7+130S^8}{384(3+2S)(4+S)(1-S)^6} \end{aligned} \tag{26}$$

where $S = \mathrm{sech}(2kh)$ [4].

B Two-wave Interaction

This appendix contains the equation for surface elevation η and the velocity potential ϕ in a two-wave interaction. The following is the equation for surface elevation η in a two-wave interaction proposed by Longuet-Higgins and Stewart [12]:

$$\eta = \eta_1 + \eta_2 + \frac{a_1 a_2}{2g}\{Ccos(\psi_1 - \psi_2) - Dcos(\psi_1 + \psi_2)\} \tag{27}$$

where

$$\psi_1 = (k_1 x - \omega_1 t)\ ;\ \psi_2 = (k_2 x - \omega_2 t) \quad . \tag{28}$$

In addition, the velocity potential is given by

$$\begin{aligned}\phi = \phi_1 + \phi_2 + \frac{E\cosh[(k_1 - k_2)(z+h)]\sin(\psi_1 - \psi_2)}{g(k_1 - k_2)\sinh(k_1 h - k_2 h) - (\omega_1 - \omega_2)^2\cosh(k_1 h - k_2 h)} \\ + \frac{F\cosh[(k_1 + k_2)(z+h)]\sin(\psi_1 + \psi_2)}{g(k_1 + k_2)\sinh(k_1 h + k_2 h) - (\omega_1 + \omega_2)^2\cosh(k_1 h + k_2 h)}\end{aligned} \tag{29}$$

where

$$\begin{aligned}C = \frac{[2\omega_1\omega_2(\omega_1 - \omega_2)(1 + \alpha_1\alpha_2) + \omega_1^3(\alpha_1^2 - 1) - \omega_2^3(\alpha_2^2 - 1)](\omega_1 - \omega_2)(\alpha_1\alpha_2 - 1)}{\omega_1^2(\alpha_1^2 - 1) - 2\omega_1\omega_2(\alpha_1\alpha_2 - 1) + \omega_2^2(\alpha_2 - 1)} \\ + \omega_1^2 + \omega_2^2 - \omega_1\omega_2(\alpha_1\alpha_2 + 1)\end{aligned} \tag{30}$$

$$\begin{aligned}D = \frac{([2\omega_1\omega_2(\omega_1 + \omega_2)(1 - \alpha_1\alpha_2) - \omega_1^3(\alpha_1^2 - 1) - \omega_2^3(\alpha_2^2 - 1)](\omega_1 + \omega_2)(1 + \alpha_1\alpha_2)}{\omega_1^2(\alpha_1^2 - 1) - 2\omega_1\omega_2(1 + \alpha_1\alpha_2) + \omega_2^2(\alpha_2 - 1)} \\ + \omega_1^2 + \omega_2^2 + \omega_1\omega_2(1 - \alpha_1\alpha_2)\end{aligned} \tag{31}$$

$$E = -\frac{1}{2}a_1 a_2[2\omega_1\omega_2(\omega_1 - \omega_2)(1 + \alpha_1\alpha_2) + \omega_1^3(\alpha_1^2 - 1) - \omega_2^3(\alpha_2^2 - 1)] \tag{32}$$

$$F = -\frac{1}{2}a_1 a_2[2\omega_1\omega_2(\omega_1 + \omega_2)(1 - \alpha_1\alpha_2) - \omega_1^3(\alpha_1^2 - 1) - \omega_2^2(\alpha_2^2 - 1)] \tag{33}$$

with

$$\alpha_1 = \frac{1}{\tanh(k_1 h)} \quad \text{and} \quad \alpha_2 = \frac{1}{\tanh(k_2 h)} \quad . \tag{34}$$

C Second Order Random Wave Theory

This appendix contains the expressions for surface elevation η and velocity potential ϕ for the second order RWT by Sharma and Dean [5]. Surface elevation is given as

$$\eta = \frac{1}{4}\sum_{i=1}^{\infty}\sum_{j=1}^{\infty} a_i a_j \Bigg\{ \left[\frac{D_{ij}^{-} - (\mathbf{k}_i \cdot \mathbf{k}_j + R_i R_j)}{\sqrt{R_i R_j}} + (R_i + R_j) \right] \cos(\psi_i - \psi_j) + \left[\frac{D_{ij}^{+} - (\mathbf{k}_i \cdot \mathbf{k}_j - R_i R_j)}{\sqrt{R_i R_j}} + (R_i + R_j) \right] \cos(\psi_i + \psi_j) \Bigg\} \quad . \tag{35}$$

The velocity potential is given by,

$$\phi = \frac{1}{4}\sum_{i=1}^{\infty}\sum_{j=1}^{\infty} b_i b_j \frac{\cosh k_{ij}^{-}(h+z)}{\cosh k_{ij}^{-} h} \frac{D_{ij}^{-}}{\omega_i - \omega_j} \sin(\psi_i - \psi_j) + \frac{1}{4}\sum_{i=1}^{\infty}\sum_{j=1}^{\infty} b_i b_j \frac{\cosh k_{ij}^{+}(h+z)}{\cosh k_{ij}^{+} h} \frac{D_{ij}^{+}}{\omega_i + \omega_j} \sin(\psi_i + \psi_j) \tag{36}$$

with

$$k_{ij}^{-} = |\mathbf{k}_i - \mathbf{k}_j| \quad \text{and} \quad k_{ij}^{+} = |\mathbf{k}_i + \mathbf{k}_j| \tag{37}$$

and

$$D_{ij}^{+} = \frac{(\sqrt{R_i} + \sqrt{R_j})\left[\sqrt{R_i}(k_j^2 - R_j^2) + \sqrt{R_j}(k_i^2 - R_i^2)\right]}{(\sqrt{R_i} + \sqrt{R_j})^2 - k_{ij}^{+} \tanh(k_{ij}^{+} h)} + \frac{2(\sqrt{R_i} + \sqrt{R_j})^2 (\mathbf{k}_i \cdot \mathbf{k}_j - R_i R_j)}{(\sqrt{R_i} - \sqrt{R_j})^2 - k_{ij}^{+} \tanh(k_{ij}^{+} h)} \tag{38}$$

$$D_{ij}^{-} = \frac{(\sqrt{R_i} - \sqrt{R_j})\left[\sqrt{R_i}(k_i^2 - R_i^2) + \sqrt{R_i}(k_j^2 - R_j^2)\right]}{(\sqrt{R_i} + \sqrt{R_j})^2 - k_{ij}^{-}\tanh\left(k_{ij}^{-}h\right)} + \frac{2(\sqrt{R_i} - \sqrt{R_j})^2(\mathbf{k}_i \cdot \mathbf{k}_j + R_i R_j)}{(\sqrt{R_i} - \sqrt{R_j})^2 - k_{ij}^{-}\tanh\left(k_{ij}^{-}h\right)} \tag{39}$$

where

$$R_i = k_i \tanh(k_i h). \tag{40}$$